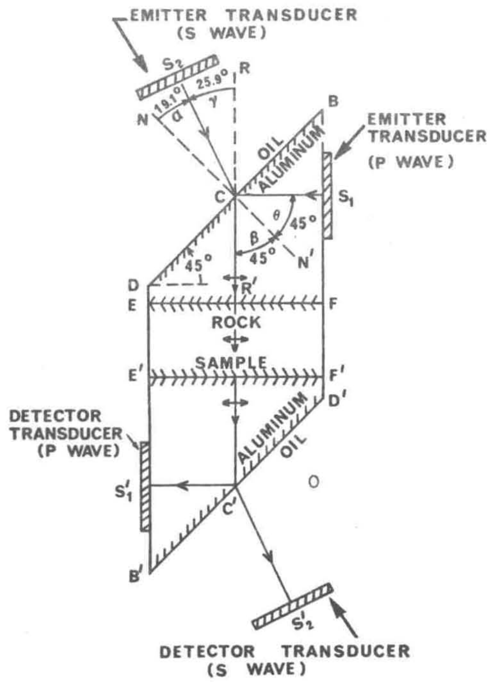

Fig. 1. Schematic diagram showing geometry and relative orientation of transducers and sample assembly.

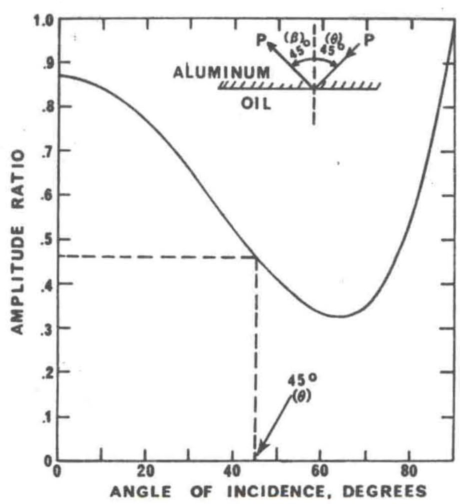

Fig. 2. Ratio of amplitude of reflected P wave to amplitude of incident P wave at aluminum–oil interface.

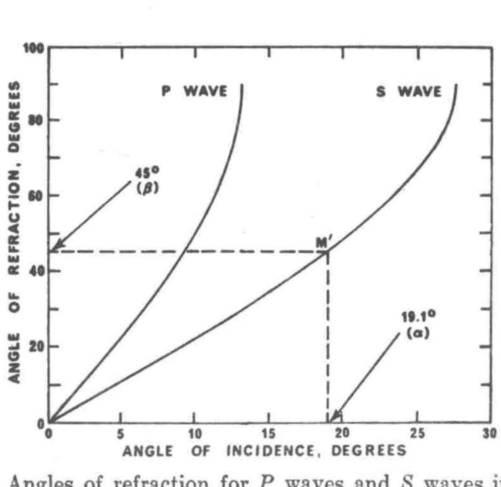

Fig. 3. Angles of refraction for P waves and S waves in aluminum for P waves incident in oil against aluminum.

travels in the compressional mode for angles of incidence less than the first critical angle. The energy of the beam is completely reflected at the first critical angle; beyond this angle a shear mode only is transmitted into the solid. Fig. 4 shows a plot of the amplitude ratios versus the angle of incidence for a refracted S wave transmitted into aluminum at an oil–aluminum interface. The curve was derived from (4) in the Appendix. Fig. 1 indicates that S waves are formed by mode conversion when P waves from transducer S_2 strike the center of the oil–aluminum interface BD at point C. The slope of the interface fixes the angle of refraction β so that the S-wave beam is directed along RR' normal to the flat aluminum–rock interface EF. The shear energy passes through the sample to the aluminum–oil interface $B'D'$, where it is converted back to a P wave at point C' and is detected by transducer S_2'. Point M' in Fig. 3 shows that the angle of incidence α is 19.1° when $\beta = 45°$. The amplitude ratio of the refracted S wave is shown at point M in Fig. 4 to be almost 0.6 when $\alpha = 19.1°$. In Fig. 1, the surfaces of transducers S_2 and S_2' are parallel, interfaces EF and $E'F'$ are flat and parallel, and angle $\gamma = \beta - \alpha$.

The flat interfaces between the aluminum wedges and the rock sample play an important role in energy transmission. The geometrical relationships between the wedge and transducers are chosen to direct both P-wave and S-wave beams at normal incidence across these interfaces. The relative amounts of energy reflected and transmitted depend primarily on the impedance match between the aluminum and the rock. Reflection and transmission coefficients are easily computed since no mode transformation occurs for the acoustic beam at normal incidence. Coefficients for P waves and S waves are given in Table I for different wedge materials in contact with samples of Boise sandstone and Solenhofen limestone. These two rocks have widely different physical properties and illustrate the marked contrast in acoustic impedance found in consolidated sedimentary type rocks. Different wedge materials are not equally effective as transmitters of acoustic energy when properties of the rock change. Aluminum transmits 99.4 percent of the P-wave energy into Solenhofen limestone but only 78.5 percent of it into Boise sandstone. Similarly, the S-wave energy transfer is 95.5 percent into Solenhofen limestone and 85.5 percent into Boise sandstone. Table I clearly shows that aluminum is superior to the other wedge materials for transmitting energy.

In the sending and receiving transducer assembly the relative orientation of the liquid–solid interfaces (mode converters) markedly influence the transformation of S waves into P waves at the receiving transducer. Shear waves are polarized and particles of the medium vibrate in a plane that contains the direction of vibration of the incident beam CC' and the direction of wave propagation $C'S_2'$. A plane-polarized S wave incident on an interface will not convert into a P wave if its direction of vibration is perpendicular to the plane containing the incident and the transmitted waves [24]. Therefore,

TABLE I
COEFFICIENTS OF REFLECTION R AND TRANSMISSION T COMPUTED FOR P-WAVE AND S-WAVE ULTRASONIC BEAMS AT NORMAL INCIDENCE TO CERTAIN WEDGE-ROCK INTERFACES*

Wedge Material	Interface Between Wedge and Dry Solenhofen Limestone				Interface Between Wedge and Dry Boise Sandstone			
	P Wave		*S* Wave		*P* Wave		*S* Wave	
	R	*T*	*R*	*T*	*R*	*T*	*R*	*T*
Brass	0.184	0.816	0.143	0.857	0.498	0.502	0.424	0.576
Aluminum (2024-T351)	0.006	0.994	0.045	0.955	0.215	0.785	0.145	0.855
Steel (SAE 4140)	0.272	0.728	0.253	0.747	0.580	0.420	0.536	0.464
Plexiglas	0.422	0.578	0.472	0.528	0.115	0.885	0.187	0.813

* Coefficients were computed from the relation $R = [(Z_2/Z_1 - 1)/(Z_2/Z_1 + 1)]^2$ where Z_1 = acoustic impedance of wedge material, Z_2 = acoustic impedance of the rock, and $R + T = 1$.

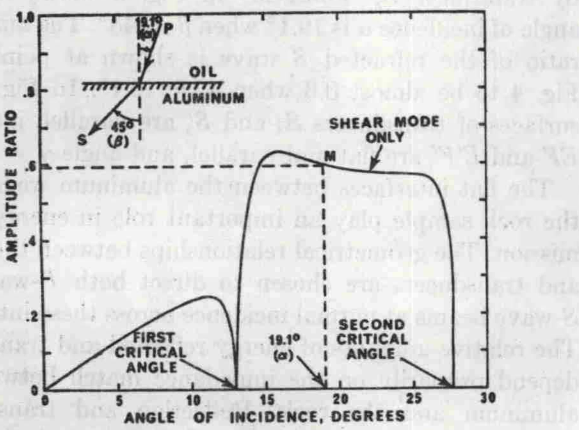

Fig. 4. Ratio of amplitude of refracted S wave to amplitude of incident P wave at oil–aluminum interface.

the best transmission through the assembly occurs when the planes of the interfaces BD and $B'D'$ are parallel (Fig. 1).

Construction and Assembly of Transducer Cells

Fig. 5 shows the construction details of one of the cells in which the transducers are mounted. One cell contains transmitting transducers, and a similar cell, receiving transducers. The cavity inside the cell contains mineral oil[1] and is sealed off at atmospheric pressure. The oil acts as a coupling medium between transducer F (S-wave source) and the aluminum wedge. Transducer G serves as the P-wave source and is spring-mounted in direct contact with the aluminum. A small air-filled bellows attached inside the cavity acts as a pressure-compensator to ensure that the pressure on the mineral oil does not change when the cell is stressed.

The piezoelectric elements, thickness-expander barium titanate disks, have diameters of 2.54 cm and resonant frequencies near 1 MHz. Other disks with frequencies between 0.25 and 5.0 MHz may be substituted and used

[1] A clear mineral oil having a density of 0.85×10^3 kg/m^3 and an acoustic velocity of 1426 m/s at 24°C and atmospheric pressure.

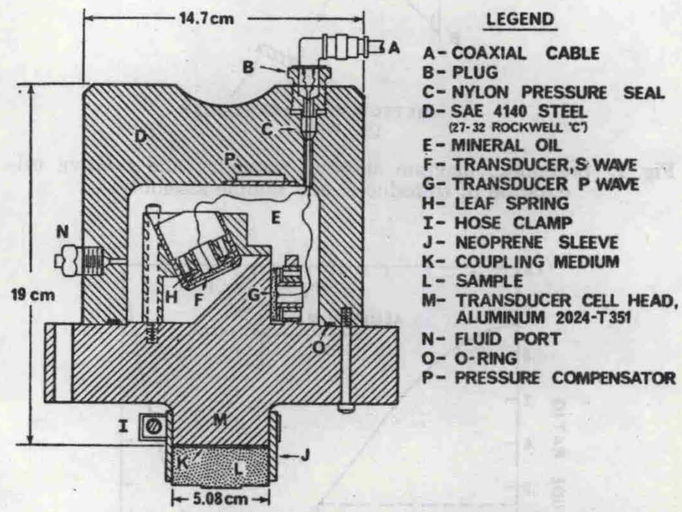

Fig. 5. Detailed cross section of transducer cell.

in the same mounts. The lower operating frequency limit is influenced by the possibilities of boundary conversions caused by beam spread as discussed by Mason [26]. The upper frequency limit is influenced by scatter caused by small ratios of wavelength λ to average particle diameter $\bar{d}p$. It was found by Grossman [27] that wave transmission was best in metals when $\lambda/\bar{d}p > 30$; transmission was greatly reduced when $\lambda/\bar{d}p < 10$. These ratios are also useful for estimating how scatter affects wave transmission in granular rocks. Results become suspect when grain dimensions approach the wavelength of the applied signal.

The transducer cells are assembled for measuring elastic-wave velocities through rock samples under triaxial loading as shown in Fig. 6. A neoprene sleeve with a wall thickness of 3.2 mm jackets the sample and serves as a flexible impermeable barrier to the hydraulic fluid. The fluid exerts pressure uniformly in the lateral and axial directions on the external surface of the sample. Additional pressure can be placed on the sample in the axial direction by the piston located at the bottom of the pressure vessel. Pressure on the pore fluid is transmitted through pore pressure lines, which are connected